Desalination and Water Treatment
www.deswater.com
doi: 10.1080/19443994.2015.1132395

(2016) 1–10

Taylor & Francis
Taylor & Francis Group

Photocatalytic degradation of methyl orange and cyanide by using TiO_2/CuO composite

Hassan Koohestani[a,*], Sayed Khatiboleslam Sadrnezhaad[b]

[a]*Faculty of Materials and Metallurgical Engineering, Semnan University, Semnan, Iran, Tel. +98 23 33654100; Fax: +98 23 33321005; email: h.koohestani@semnan.ac.ir*
[b]*Department of Materials Science and Engineering, Sharif University of Technology, Azadi Ave., Tehran, Iran, email: sadrnezh@yahoo.com*

Received 3 September 2015; Accepted 28 November 2015

ABSTRACT

In this study, the effect of adding 5–12.5 wt% CuO to TiO_2 on photocatalytic properties of the nano-composite TiO_2/CuO was investigated. The products were characterized by X-ray diffractometer, SEM, Brunauer–Emmett–Teller (BET), and DRS. BET-specific surface area of the TiO_2/CuO composites was lower than that of the pure TiO_2. Incorporation of CuO into TiO_2 shifted absorption spectra to the visible region. As the CuO content increased from 0 to 12.5%, a clear decrease in optical band gap from 2.95 to 2.30 eV was observed. The photocatalytic performance was determined by methyl orange degradation and cyanide photo-oxidation under ultraviolet irradiation. However, the excessive incorporation of CuO did not improve any ability of TiO_2 to degrade MeO and cyanide. The highest rate of photocatalytic degradation was found in TiO_2–7.5% CuO. The rate constants of the dye degradation reaction using TiO_2 and TiO_2–7.5% CuO catalysts were 0.0107 and 0.0151 min^{-1}, respectively. Corresponding results for cyanide disinfection were 0.0049 and 0.0110 min^{-1}.

Keywords: TiO_2/CuO; Photodegradation; Nano-composite; Cyanide; Methyl orange

1. Introduction

Wastewater discharged by industrial activities is often contaminated with a variety of toxic or other harmful substances which have a negative effect on the water environment [1]. These include organic chemicals, inorganic chemicals, and heavy metals [2].

Textile dyes and cyanide (CN) are toxic chemical compounds present in industrial effluents that represent an increasing environmental danger [3,4]. Over 50% of all the dyes used in various industries are azo dyes, which are characterized by one or more azo bonds (−N=N−). Due to high concentration of organics in the effluents and higher stability of synthetic dyes, their discharges into water are harmful to humans and animals [3,5]. Cyanide (CN) is a highly toxic component, which is generated from several industrial activities such as gas production, pharmaceutical, mining, electroplating processes, and coal gasification [4]. Owing to their toxicity, it is necessary to purify wastewaters containing cyanide before directing them to the receiving waters [4,6].

Different methods such as flocculation, the chemical oxidation including Fenton's reagent, O_3, etc., air floatation processes, adsorption processes, and anaerobic–aerobic two-stage biochemical process have

*Corresponding author.

been used to remove different pollutants from water and especially wastewaters [1,3,7]. They just transfer organic compounds from water to another phase, thus causing secondary pollution. Consequently, regeneration of the adsorbent materials and post-treatment of solid wastes, which are expensive operations, are needed [3,6].

Recently, advanced oxidation processes (AOPs), based on the production of highly reactive hydroxyl radicals, have been proposed as an efficient method for the removal of different pollutants [4,8]. Heterogeneous photocatalysis based on semiconductors is the most famous AOP, in which irradiating the semiconductor by photons with sufficient energy with respect to the band gap energy of the semiconductor produces electron/hole pairs. The produced electron/holes can generate reactive hydroxyl or super oxide radicals by reaction of electron/hole with water and dissolved molecular oxygen, which can destroy different organic pollutants to smaller fragments and finally to water and CO_2 [8–10].

Among the various semiconductor materials, TiO_2 has been widely studied due to its favorable physical/chemical properties, low cost, chemical stability, and non-toxicity. However, the practical applications of TiO_2 have been suppressed because of its two drawbacks. One of which is the rapid recombination of photo-induced electrons and holes and the other is the poor solar efficiency, which is determined by its band gap [11,12].

A number of strategies have been devised to bring about the modifications in electronic structure of titania, with a view to overcome the drawbacks mentioned earlier. These include doping with metals and coupling with other semiconducting oxides [11,13].

Nanostructured composite materials have been fundamentally studied and widely applied in a number of areas. The electron transfer between TiO_2 and other materials brings new performances to TiO_2-based composite [14]. Among various oxides, transition metals have attracted considerable attention due to their interesting photochemical and photomagnetic properties [15].

It has been reported that CuO, p-type semiconductor, with a narrow band gap (E_g = 1.2–1.5 eV) has potential applications in many fields such as high-critical-temperature superconductors, photovoltaic materials, field emission, and catalysis [5,7,16,17]. Meanwhile, TiO_2/CuO nanoparticles have also been reported to show enhanced degradation of organic pollutants owing to their modified optical property which has enabled the composite material to tap into the visible light range of the solar irradiation [18]. The high catalytic activity was attributed to photo-excitation of electrons in the conduction bands of both CuO and TiO_2, followed by migration of the conduction band electrons in TiO_2 into the conduction band of CuO [19]. The accumulation of excess electrons in the conduction band of CuO caused a negative shift in the Fermi level of CuO to provide the required overvoltage necessary for efficient water reduction [19,20].

In this study, TiO_2/CuO nanocomposites were successfully synthesized. Then, CuO was loaded on TiO_2, and its effect on the photocatalytic activity was investigated by degrading methyl orange (MeO) and cyanide. Decolorization of MeO, a stable azo dye, by UV irradiation in the presence of composites was verified by UV–vis spectrophotometer. The remaining concentration of cyanide was analyzed by the titration method. The structural and optical properties of the samples were studied by X-ray diffractometer (XRD), SEM, Brunauer–Emmett–Teller (BET), and UV–vis DRS spectra and then compared with each other.

2. Exprimental

2.1. Materials

Titanium(IV) isopropoxide (TTIP), copper(II) sulfate ($CuSO_4{\cdot}5H_2O$), sodium hydroxide (NaOH), ascorbic acid ($C_6H_8O_6$), ethanol (98%), hydrochloric acid (HCl), 2-propanol, methyl orange ($C_{14}H_{14}N_3NaO_3S$), potassium cyanide (KCN), and ethylenediaminetetraacetic acid (EDTA) were purchased from MERCK manufacturer.

2.2. Synthesis

The TTIP and $CuSO_4{\cdot}5H_2O$ were used as titania and CuO precursor for synthesizing TiO_2, CuO, and TiO_2/CuO nanoparticles. The CuO and titania precursor solutions were prepared separately.

2.2.1. Solution A

CuO precursor solution was obtained by dissolving 0.4 g of $CuSO_4{\cdot}5H_2O$ in 100 mL of deionized water and magnetic stirred for 20 min. Then, 30 mL of 0.05 M NaOH was added in dropwise manner into the solution. After stirring for 30 min, 30 mL of 0.05 M ascorbic acid solution was dropped into the solution, and the color of precipitates gradually changed from blue to brick red.

2.2.2. Solution B

The titania precursor solution was obtained by mixing distilled water (85 mL), HCl (6 mL), and

2-propanol (6 mL) at room temperature. Then, titanium isopropoxide (5 mL) was gradually added to the solution. The mixture was stirred for 120 min at 60°C.

In order to obtain TiO_2/CuO nano-composite, solution **A** was added in solution **B** in which the CuO molar ratio was adjusted to many values (5, 7.5, 10, and 12.5%). Finally, all samples were calcined at 450°C for 120 min in the furnace.

2.3. Characterization

The crystalline structure was obtained using a X-ray diffractometer (XRD, Spectro Xepos, Germany) with monochromated high-intensity Cu Kα radiation (λ = 1.5418 Å). Scherrer equation which is well used to measure the crystal size according to the XRD pattern was adopted for the estimation of nano-crystalline size. The morphology of the samples was studied using a field-emission scanning electron microscope (FESEM, Mira 3-XMU, Czech).

The BET-specific surface area was determined using a Belsorp mini II (Japan) system. The diffusive reflectance spectra (DRS) of the samples were recorded by a UV–vis spectrophotometer (Avaspec-2048-TEC, Netherlands) using $BaSO_4$ as a reference in the region from 200 to 900 nm.

2.4. Photocatalytic degradation

2.4.1. Methyl orange

Catalytic activity of the samples was estimated from color degradation of the methyl orange aqueous solution (50 mL MeO with 5 mg L^{-1} initial concentration). The pH was maintained constant, equal to the initial pH of the MeO solution (i.e. 6.5). The same amount of catalyst was used (150 mg L^{-1}). Before irradiation with UV light, the aqueous solution which contained TiO_2 catalyst was continuously stirred for 60 min in full darkness to achieve adsorption–desorption equilibrium. UV irradiation from two 6 W lamp (Philips, China) was then applied to the catalyst containing solution. The distance between the surface of the solution and the light source was 10 cm. Samples were then taken out for analysis, every 30 min.

Solution concentration was determined by UV–vis spectrophotometer (6705; Jenway, UK). The maximum absorption wavelength registered for MeO was 462 nm.

The efficiency of degradation (η%) was calculated from the Eq. (1) [9]:

$$\eta\% = \left(\frac{C_0 - C}{C_0}\right) \times 100 \quad (1)$$

where C_0 and C are initial and time-dependant concentrations of the dye, respectively.

2.4.2. Cyanide

Sample solution of cyanide was prepared by dissolving KCN into deionized water (100 mg L^{-1}). Photocatalytic experiments were performed with pH 10, constant temperature (25°C), and contact time of 0–180 min in the presence of 100 mg L^{-1} EDTA as sacrificial reagent.

After the equilibration period (60 min in the dark), the UV-lamps (two 6 W lamps; Philips, China) were turned on. The remaining concentration of cyanide was analyzed by 4500-CN D. Titrimetric Method according to Standard Methods for the Examination of Water and Wastewater. Then, residual cyanide concentration was calculated using the following equation [21,22]:

$$\frac{\text{mg } CN^-}{\text{L}} = \frac{(A - B) \times 1000}{\text{mL orginal sample}} \times \frac{250}{\text{mL portion used}} \quad (2)$$

where A and B is volume (mL) of standard $AgNO_3$ of sample and of blank, respectively.

3. Result and discussion

The XRD patterns of TiO_2 and CuO samples having been calcined at 450°C are shown in Fig. 1. The XRD pattern of TiO_2 is shown in Fig. 1(a), which exhibits both phases, anatase (identified with JCPDS: 00-021-1272) and rutile (identified with JCPDS: 00-021-1276) characteristic peaks. Using the Scherer equation, the average crystallite sizes of anatase and rutile were estimated to be 16.4 and 19.7 nm, respectively. The fraction of the crystalline phases was determined by integrating the relative intensities of the anatase (1 0 1) (2θ = 25.4°) and the rutile (1 1 0) (2θ = 27.5°) peaks [23]:

$$W_A = \frac{1}{1 + 1.26\frac{I_R}{I_A}} \quad (3)$$

where W_A is the weight fraction of the anatase and I_A and I_R represent the integrated intensities of the anatase (1 0 1) and the rutile (1 1 0) peaks, respectively.

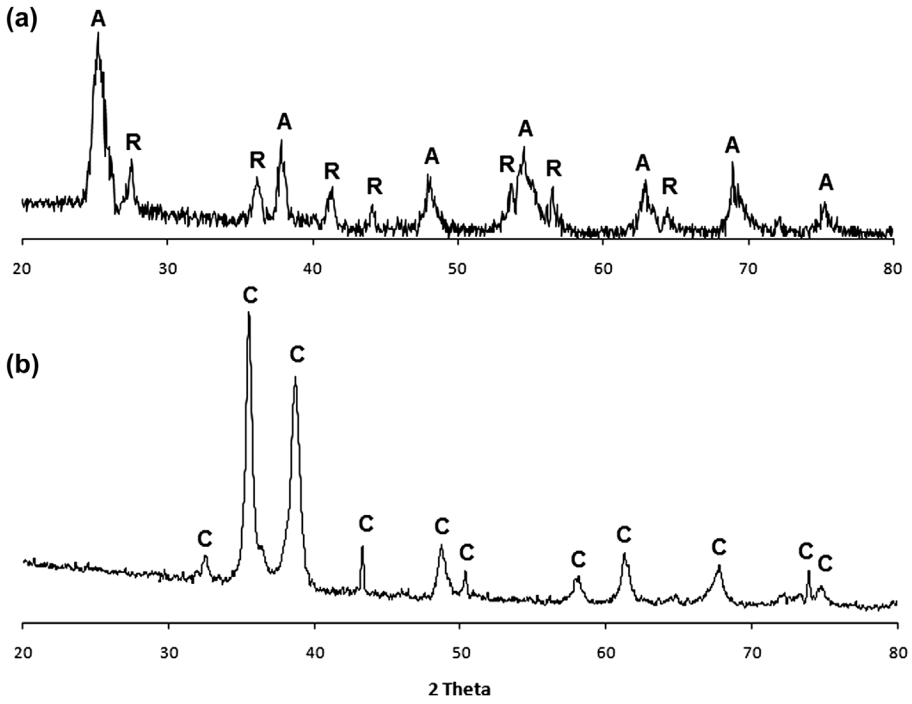

Fig. 1. X-ray diffraction patterns of (a) TiO_2 and (b) CuO.

From Eq. (3), the fraction of the anatase in our sample was 0.73.

In Fig. 1(b), for CuO, all diffraction peaks can be indexed to a crystalline monoclinic structure of CuO nanoparticles (identified with JCPDS: 00-048-1548). No other crystalline forms of copper oxide (i.e. Cu_2O) were presented, indicating that copper existed as CuO crystal after calcination at 450˚C. This result is in agreement with previous reports [24,25]. The average crystalline size of CuO nanoparticles was found to be 21.2 nm.

The XRD patterns of the TiO_2 composite powders with 5–12.5 wt% of CuO are also presented in Fig. 2. In all patterns, peaks of anatase, rutile, and relatively weak peaks of CuO can be observed. A few reports have attributed the weak peak of CuO to the low Cu content and high dispersion of the Cu species within the photocatalysts [18]. The average crystallite sizes of sample phases calcined at 450˚C are summarized in Table 1. It can be seen that as CuO content increases, although CuO crystallite sizes become bigger, there is a small increase in anatase and rutile crystallite sizes.

Fig. 3 displays SEM images of the pure TiO_2 and TiO_2–7.5% CuO particles. The photocatalysts consisted of relatively irregular and spherical particles. Particle size of TiO_2 and TiO_2–7.5% CuO was 20–30 and 30–50 nm, respectively. One can see that composite particles are bigger than pure TiO_2. Perazolli et al. [20] reported that CuO presence increases catalysts' particle size and causes particles to agglomerate. Energy-dispersive X-ray (EDX) analysis of the TiO_2–7.5% CuO composite is shown in Fig. 3(c) and (d). The EDXs have been taken from different parts of the SEM image and are presented in the figure. They indicated three elements of titanium, oxygen, and copper on the surface of the annealed sample.

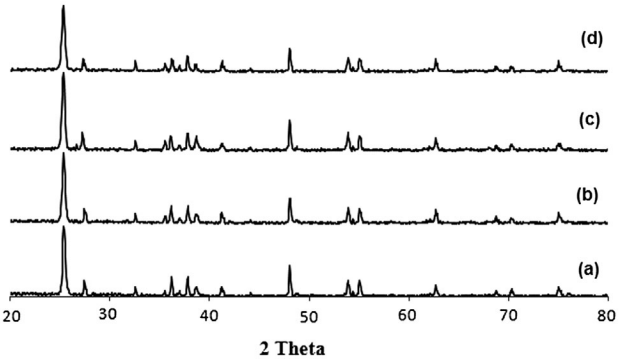

Fig. 2. XRD patterns of TiO_2/CuO with variation of CuO content (a–d: 5.0, 7.5, 10.0, and 12.5 wt%).

The BET-specific surface area of synthesized samples is listed in Table 2. As depicted, the BET-specific surface area of the TiO_2/CuO composites was significantly lower than that of the pure TiO_2. This could be

Table 1
The crystal phase and the average crystallite size of TiO_2/CuO samples

	Crystallite size (nm)		
% CuO	Anatase	Rutile	CuO
0	16.4	19.7	0
5	16.0	19.8	20.2
7.5	15.9	19.8	20.5
10	16.1	19.7	21.4
12.5	16.8	19.9	22.1

ascribed to the occupied surface area on the TiO_2 by CuO nanoparticles as well as agglomeration of TiO_2 nanoparticles which have resulted in the reduced available surface area for adsorption [26]. This was consistent with the formation of bigger TiO_2 crystals and hence a lower specific surface area, due to the addition of CuO. Among composites, the sample containing 10% CuO with 65.5 $m^2 g^{-1}$ shows a larger specific surface area compared to that of others.

The photocatalytic performance of a semiconductor significantly depends on its optical property, and thus, it is one of the important factors which should be

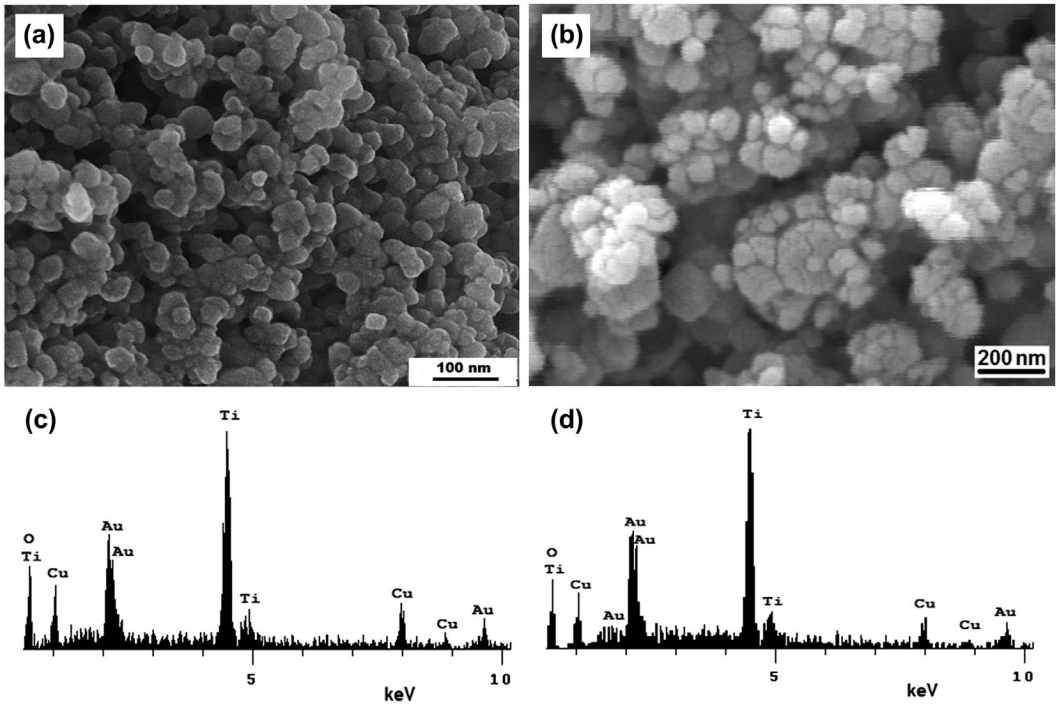

Fig. 3. SEM images: (a) TiO_2 and (b) TiO_2–7.5% CuO, EDX diagrams: (c) and (d) TiO_2–7.5% CuO calcined at 450°C.

Table 2
Physical properties and photocatalytic performance of the synthesized TiO_2/CuO photocatalysts

			Methyl orange		Cyanide	
Photocatalyst	BET-specific surface area ($m^2 g^{-1}$)	Band gap energy, E_g (eV)	k (min^{-1})	R^2	k (min^{-1})	R^2
TiO_2	68.2	2.95	0.0107	0.987	0.0049	0.895
TiO_2–5% CuO	60.3	2.68	0.0110	0.969	0.0056	0.978
TiO_2–7.5% CuO	57.8	2.53	0.0151	0.988	0.0110	0.973
TiO_2–10% CuO	65.5	2.50	0.0123	0.976	0.0089	0.984
TiO_2–12.5% CuO	52.1	2.30	0.0075	0.962	0.0042	0.976
CuO	56.7	–	0.0021	0.988	0.0013	0.938

studied. Fig. 4 shows typical UV–vis diffuse reflectance spectroscopy (UV–vis DRS) curves for optical absorption behavior of TiO_2/CuO samples. The optical transitions in semiconductor materials are believed to take place via direct and indirect transitions which can be studied using the following Kubelka–Munk equation [27,28]:

$$(\alpha h\nu) = \beta\left(h\nu - E_g\right)^n \tag{4}$$

where E_g is energy band gap of semiconductors (eV), ν is the frequency of light (s^{-1}), h is Planck's constant (J s), β is the absorption constant, and α is the absorption coefficient defined by the Beer–Lambert law as $\alpha = ([2.303 \times Abs]/d)$, where d and Abs are the sample thickness and sample absorbance, respectively. For precise determination of α, some corrections should be made to the absorption due to reflection. In this equation, index n has different values of 1/2, 2, 3/2, and 3 for allowed direct, allowed indirect, forbidden direct, and forbidden indirect electronic transitions [27,28].

The band gap can be determined by extrapolating the linear portion of the $(\alpha h\nu)^n$–$h\nu$ curve. The best linear fitting was obtained for the $(\alpha h\nu)^{0.5}$–$h\nu$ curve for the TiO_2/CuO catalyst which is in accordance with the literature for both semiconductors.

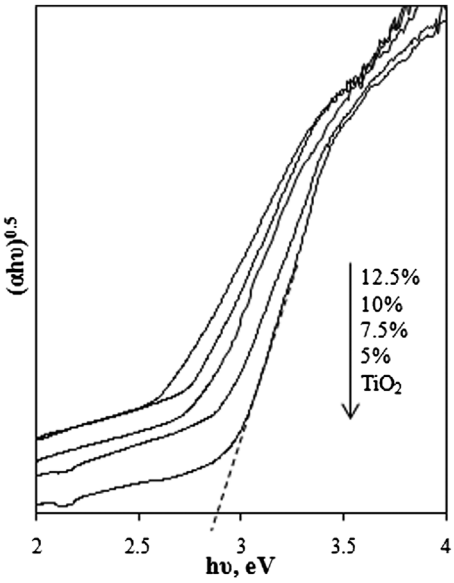

Fig. 4. The corresponding Kubelka–Munk function spectra to determine indirect new band gap values for the synthesized TiO_2/CuO photocatalysts with variation of CuO content. The UV–vis spectra of the synthesized photocatalysts with variation of CuO content (a–e: 0, 5.0, 7.5, 10.0, and 12.5 wt%) calcined at 450˚C.

In general, increasing the CuO content has resulted in the increase in the absorption intensity in the UV and visible light regions. The red-shifting was attributed to the additional energy levels created by the Cu ions in the band gap of TiO_2 [29,30]. Table 2 summarizes the results of band gap energy of all the photocatalysts obtained from the UV–vis absorption spectra and Eq. (4). The results show that the band gap energy decreased with increasing CuO ratio; that is, it increased from 2.95 eV for the pure TiO_2 to 2.30 eV for the TiO_2–12.5% CuO composite.

There exists a transition from the valence band of the CuO to the conduction band of TiO_2, thus resulting in the significant narrowing of the TiO_2 band gap energy. This implies that the electronic structures of the pristine TiO_2 have been modified via the formation of the TiO_2/CuO heterojunctions. It can be suggested as a reduction in the band gap energy of the TiO_2/CuO, which could lead to an increase in the quantity of the electron/hole formation and recombination.

The photocatalytic activity of samples was measured by the degradation efficiency of MeO solution without concerning the degradation intermediates in detail. The degradation efficiency of MeO solution versus photocatalytic time under UV–vis irradiation is illustrated in Fig. 5.

It is evident that CuO is a photocatalyst that can absorb the light from the UV to visible region. However, single CuO material has poor photocatalytic activity due to its low charge-transfer rate. And the amount of degradation in its presence was obtained as approximately 60% after 210 min. But concerning the result, it is clear that CuO was an excellent co-catalyst with TiO_2, due to enhanced charge separation and

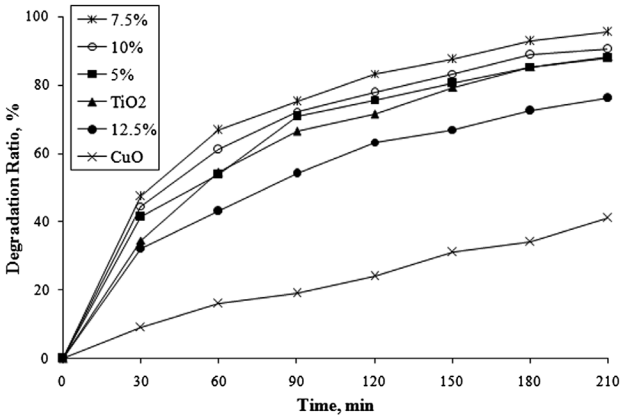

Fig. 5. Comparison of the degradation efficiency of MeO in the presence of synthesized catalysts and under UV–vis light irradiation.

oxygen reduction in the interfaces between the two coupled catalysts.

The catalytic efficiency increased with the increase in CuO amount on TiO_2 in a certain range (5–7.5 wt%), but decreased at higher CuO loading (10 and 12.5 wt %). In general, the greater amount of CuO produces more generated holes and hydroxyl radicals [5,17]. The maximum photocatalytic activity was achieved for composite sample containing 7.5% CuO. It is known that the photocatalytic redox reaction mainly occurs on the surface of the photocatalysts, so the surface properties significantly influence the efficiency of photocatalysts. The decolorization rate at higher CuO loadings beyond optimum level (7.5% of CuO) decreased. At higher values, because of deactivation of activated CuO species due to meeting ground state one, generation of hydroxyl radicals and hence the degradation efficiency were decreased [5,17]. In addition, the formation of CuO aggregates shields the incident light intensity, reduces the adsorption capacity of the support, and consequently decreases the photocatalytic activity. Aggregation can also reduce the specific area of photocatalyst, providing less active site for the light and pollutant introducing [17,31].

Huang et al. [32] and Moon et al. [33] reported that the best catalytic effect was achieved when the amount of CuO was near the monolayer dispersion threshold, in higher amounts of CuO loading, the number of the effective active phase species was reduced with the increase in crystalline CuO, resulting in a suppression of catalytic activity. Other reasons for the dual effect of copper oxide on photocatalytic performance of TiO_2 are (i) opacity and light scattering of TiO_2 by CuO resulting in a decreased passage of irradiation [24] and (ii) increase in nanodot size leading to deterioration of photocatalytic activity [33]. The similar results were reported by Li et al. [34] who pointed out that beyond a critical quantity, any additional copper loading was in the form of bulk crystalline oxide.

Fig. 6 displays that the photocatalytic degradation corresponds to a pseudo-first-order reaction. Pseudo-first-order kinetics was assumed to calculate the corresponding degradation rate constant (k) [5]:

$$\ln\left(\frac{C}{C_0}\right) = -kt \tag{5}$$

where C_0 is the original MeO concentration after the adsorption/desorption reached equilibrium (mg L^{-1}), C is the concentration (mg L^{-1}) at a given time t (min), and k is the first-order degradation rate constant (min^{-1}). Table 2 lists the results of kinetic analysis of

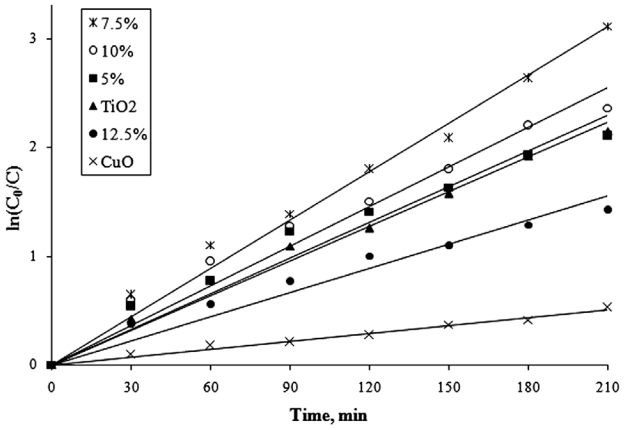

Fig. 6. First-order kinetics for the MeO photodegradation on the synthesized photocatalysts with variation of CuO content.

MeO degradation. The obtained linear regression coefficients (R^2) were relatively high, indicating that the photocatalytic decolorization of MeO obeys the Langmuir–Hinshelwood (first-order) kinetic model. It was found that the rate constant of TiO_2 increased with the presence of CuO. At 7.5% CuO, the reaction rate constant (0.0151 min^{-1}) was larger than that of TiO_2 alone (0.0107 min^{-1}). Therefore, when CuO content was 7.5%, the degradation rate was the highest among the other composites.

In the cyanide removal, the mechanism is based on the absorption of light energy by the semiconductor particles which must be of a wavelength sufficient to exceed the band gap energy of the semiconductor to produce electron/hole pairs (e^-–h^+). From the reaction of cyanide ion with positive hole, CN^- is oxidized to OCN^-, while oxygen is photoreduced to hydrogen peroxide by photogenerated electrons in the conduction band of photocatalysts. Thus, the process to remove CN^- can be represented as follows [21,35,36]:

$$TiO_2 + 2h\nu = TiO_2(2h^+ + 2e^-) \tag{6}$$

$$1/2\ O_2 + 2e^- + H_2O = 2OH^- \tag{7}$$

$$2OH^- + 2h^+ = 2OH^{\cdot} \tag{8}$$

$$CN^- + 2OH^{\cdot} = OCN^- + H_2O \tag{9}$$

$$2OCN^- + O_2 = 2CO_2 + N_2 \tag{10}$$

Fig. 7 shows the efficiency of photocatalytic degradation of cyanide solution by TiO_2/CuO catalysts with different wt% of CuO upon UV–vis light illumination. A sacrificial reagent (example EDTA) helps to control

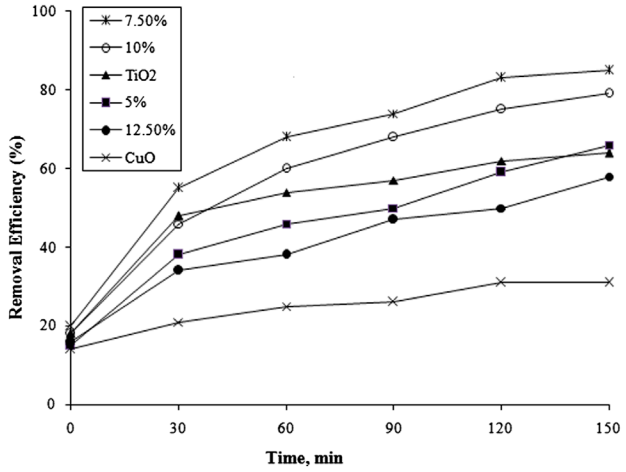

Fig. 7. The influence of CuO content on the photocatalytic degradation of cyanide by TiO_2.

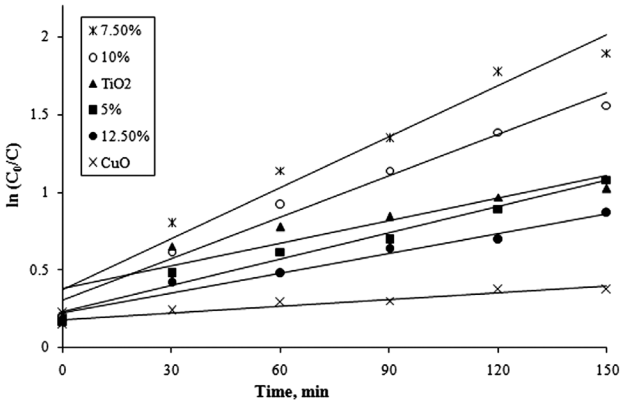

Fig. 8. First-order kinetic model for cyanide removal by TiO_2/CuO composites.

the electron/hole recombination process. The photo efficiency of the process can be improved by the addition of sacrificial reagents. The sacrificial reagents help separation of the photoexcited electrons and holes [37]. The figure indicates that the photocatalytic efficiency of pure TiO_2 does not exceed 68% after 150 min reaction time. As the band gap decreases with the increased wt% of CuO, the efficiency of the photodegradation increases sharply along with rapid decrease in time needed for the complete reaction. Looking at Fig. 7 again, one can choose 7.5 wt% CuO as optimum combination to achieve maximum efficiency after 150 min.

Since the initial concentration of cyanide employed in this study was low, the adsorption kinetics can be described adequately by a simplified first-order rate equation (Eq. (5)), where C_0 and C are the cyanide concentration at the initial time and at time t, respectively [36].

Ibrahim et al. reported that the reaction kinetic of photocatalytic decomposition of cyanide using TiO_2/SiO_2 was found to be of first order, and rate of photocatalytic degradation of cyanide using TiO_2/SiO_2 is much faster than using ozone process. Farrokhi et al. [4] suggested that photocatalytic reaction with TiO_2/UV can be effectively applied to treat industrial wastewater contaminated with cyanide. Photocatalytic oxidation rate of cyanide was well described by the first-order kinetics.

The plots of $\ln[C_0/C]$ vs. time from kinetic degratadation data on Fig. 7 are presented in Fig. 8 and results of cyanide removal are included in Table 2. The results indicate that photodegradation in the presence of TiO_2/CuO photocatalysts kinetics was satisfactorily fit to a first-order rate law. Moreover, the rate constant is increased from 0.0049 min^{-1} for TiO_2 to 0.0110 min^{-1} for TiO_2–7.5% CuO.

The role of Cu^{2+} is therefore to act simply as an electron trap and the electron has to be consumed in some way, otherwise there will be an accumulation of charge on the surface [38]. One pathway which accounts for the disappearance of a trapped electron is by the recombination reaction with the photogenerated hole from the TiO_2. Trapped electrons could also be consumed via the reduction of adsorbed oxygen molecules which is believed to be one of the rate-determining steps in TiO_2-based photocatalytic reactions [39]. If oxygen is present in the system, the Cu^+ could be oxidized back to Cu^{2+}. As a result of the $Cu^{2+} \xrightarrow{e^-} Cu^+ \xrightarrow{O_2} Cu^{2+}$ sequential reactions, the electron/hole recombination rate could be reduced [32,38].

Since the copper oxide is confined in the surface of the TiO_2, at high loading of copper oxide, there will be a high possibility for the trapped electrons to recombine with the holes. The oxidation of Cu^+ to Cu^{2+} by the photogenerated holes is expected to be faster than the oxidation of CN^- ion, since the former is simply a direct transfer of the trapped electron from Cu^+ to the valence band hole. In that case, the Cu^+ might act as a recombination center and promote the recombination reaction [34,38].

4. Conclusions

In this work, TiO_2/CuO composites were produced from a synthesized raffinate. The composites were characterized by XRD, SEM, BET, and DRS. Although the presence of CuO shifted absorption spectra to the visible region, it decreased specific surface area and increased particles' size. Their photocatalytic properties were determined from MeO

degradation data obtained from color change and solution composition alteration. Also, the photo-oxidation of cyanide by the synthesized composites was compared. The photocatalytic activity of TiO_2 increased with the increase in CuO amount to 7.5 wt %. Further increase in the CuO content beyond 7.5% considerably reduced the photocatalytic activity of TiO_2. The high concentration of nanosized CuO would cover the surface of TiO_2 leading to a drastic decrease in photon absorption and promotes the recombination of photogenerated holes with the trapped electrons resulting in a decrease in photocatalytic activity.

References

[1] L. Monser, N. Adhoum, Modified activated carbon for the removal of copper, zinc, chromium and cyanide from wastewater, Sep. Purif. Technol. 26 (2002) 137–146.

[2] S.R. Wild, T. Rudd, A. Neller, Fate and effects of cyanide during wastewater treatment processes, Sci. Total Environ. 156 (1994) 93–107.

[3] I.K. Konstantinou, T.A. Albanis, TiO_2-assisted photocatalytic degradation of azo dyes in aqueous solution: Kinetic and mechanistic investigations, Appl. Catal. B: Environ. 49 (2004) 1–14.

[4] M. Farrokhi, J.K. Yang, S.M. Lee, M.S. Siboni, Effect of organic matter on cyanide removal by illuminated titanium dioxide or zinc oxide nanoparticles, J. Environ. Health. Sci. Eng. 11 (2013) 1–8.

[5] A. Nezamzadeh-Ejhieh, H. Zabihi-Mobarakeh, Heterogeneous photodecolorization of mixture of methylene blue and bromophenol blue using CuO-nano-clinoptilolite, J. Ind. Eng. Chem. 20 (2014) 1421–1431.

[6] J. Aguado, R.V. van Grieken, M.J. López-Muñoz, J. Marugán, Removal of cyanides in wastewater by supported TiO_2-based photocatalysts, Catal. Today 75 (2002) 95–102.

[7] A. Nezamzadeh-Ejhieh, M. Amiri, CuO supported Clinoptilolite towards solar photocatalytic degradation of p-aminophenol, Powder Technol. 235 (2013) 279–288.

[8] A. Nezamzadeh-Ejhieh, M. Bahrami, Investigation of the photocatalytic activity of supported ZnO–TiO_2 on clinoptilolite nano-particles towards photodegradation of wastewater-contained phenol, Desalin. Water Treat. 55 (2015) 1096–1104.

[9] S. Khameneh-Asl, S.K. Sadrnezhaad, M. Keyanpour-Rad, Photocatalytic decolorization of Red Dye in aqueous ZnO–TiO_2 Suspensions, Adv. Mater. Res. 55 (2008) 577–580.

[10] B. Czech, Effect of H_2O_2 addition on phenol removal from wastewater using TiO_2/Al_2O_3 as photocatalyst, Polish J. Environ. Stud. 18 (2009) 989–993.

[11] L.R. Hou, C.Z. Yuan, Y. Peng, Synthesis and photocatalytic property of SnO_2/TiO_2 nanotubes composites, J. Hazard. Mater. 139 (2007) 310–315.

[12] A.H. Jawad, A.F. Alkarkhi, N.S.A. Mubarak, Photocatalytic decolorization of methylene blue by an immobilized TiO_2 film under visible light irradiation: Optimization using response surface methodology (RSM), Desalin. Water Treat. 2014 (2014) 1–12.

[13] V. Jeyalakshmi, R. Mahalakshmy, K.R. Krishnamurthy, B. Viswanathan, Titania based catalysts for photoreduction of carbon dioxide: Role of modifiers, Indian, J. Chem. A Inorg. Phys. Theor. Anal. 51 (2012) 1263–1283.

[14] L. Xiong, F. Yang, L. Yan, N. Yan, X. Yang, M. Qiu, Y. Yu, Bifunctional photocatalysis of TiO_2/Cu_2O composite under visible light: Ti^{3+} in organic pollutant degradation and water splitting, J. Phys. Chem. Solids 72 (2011) 1104–1109.

[15] T. H. Nguyen, T. L. Nguyen, T. D. T Ung, Q. L. Nguyen, Synthesis and characterization of nano-CuO and CuO/TiO_2 photocatalysts, Adv. Natural Sci.: Nanosci. Nanotechnol. 4 (2013) 1–6.

[16] Y. Fang, Y.R. Wang, G. Jiang, H. Jin, Y. Wang, X. Sun, S. Wang, T. Wang, CuO/TiO_2 nanocrystals grown on graphene as visible-light responsive photocatalytic hybrid materials, Bull. Mater. Sci. 35 (2012) 495–499.

[17] A. Nezamzadeh-Ejhieh, M. Karimi-Shamsabadi, Comparison of photocatalytic efficiency of supported CuO onto micro and nano particles of zeolite X in photodecolorization of Methylene blue and Methyl orange aqueous mixture, Appl. Catal. A: Gen. 477 (2014) 83–92.

[18] S.S. Lee, H. Bai, Z. Liu, D.D. Sun, Novel-structured electrospun TiO_2/CuO composite nanofibers for high efficient photocatalytic cogeneration of clean water and energy from dye wastewater, Water Res. 47 (2013) 4059–4073.

[19] W.-T, Chen, V. Jovic, D. Sun-Waterhouse, H. Idriss, G.I.N. Waterhouse, The role of CuO in promoting photocatalytic hydrogen production over TiO_2, Int. J. Hydrogen Energy. 38 (2013) 15036–15048.

[20] L. Perazolli, L. Nuñez, M.R.A. da Silva, G.F. Pegler, A.G.C. Costalonga, R. Gimenes, M.M. Kondo, M.A.Z. Bertochi, TiO_2/CuO films obtained by citrate precursor method for photocatalytic application, Mater. Sci. Appl. 2 (2011) 564–571.

[21] H. Koohestani, S.K. Sadrnezhaad, Photocatalytic activity of immobilized geometries of TiO_2, J. Mater. Eng. Perform. 24 (2015) 2757–2763.

[22] E.W. Rice, A.P.H. Association, Standard Methods for the Examination of Water and Wastewater, American Public Health Association, Washington, DC, 2012.

[23] L. Andronic, D. Andrasi, A. Enesca, M. Visa, A. Duta, The influence of titanium dioxide phase composition on dyes photocatalysis, J. Sol–Gel. Sci. Technol. 58 (2011) 201–208.

[24] E. Morrison, D. Gutiérrez-Tauste, C. Domingo, E. Vigil, J.A. Ayllón, One step room temperature photodeposition of Cu/TiO_2 composite films and its conversion to CuO/TiO_2, Thin Solid Films 517(19) (2009) 5621–5624.

[25] X. Liu, Z. Li, Q. Zhang, F. Li, T. Kong, CuO nanowires prepared via a facile solution route and their photocatalytic property, Mater. Lett. 72 (2012) 49–52.

[26] S.D. Wu, Y.Q. Zhu, C. Li, Y.L. Wei, A novel CuO–TiO_2 composite photocatalyst and its degradation of methyl orange under UV irradiation, Adv. Mater. Res. 295–297 (2011) 1129–1132.

[27] S. Azimi, A. Nezamzadeh-Ejhieh, Enhanced activity of clinoptilolite-supported hybridized PbS–CdS semiconductors for the photocatalytic degradation of a mixture of tetracycline and cephalexin aqueous solution, J. Mol. Catal. A: Chem. 408 (2015) 152–160.

[28] Z. Khodami, A. Nezamzadeh-Ejhieh, Investigation of photocatalytic effect of ZnO–SnO_2/nano clinoptilolite system in the photodegradation of aqueous mixture of 4-methylbenzoic acid/2-chloro-5-nitrobenzoic acid, J. Mol. Catal. A: Chem. 409 (2015) 59–68.
[29] Y. Wang, W. Duan, B. Liu, X. Chen, F. Yang, J. Guo, The effects of doping copper and mesoporous structure on photocatalytic properties of TiO_2, J. Nanomater. 2014 (2014) 1–7.
[30] L. Yu, S. Yuan, L. Shi, Y. Zhao, J. Fang, Synthesis of Cu^{2+} doped mesoporous titania and investigation of its photocatalytic ability under visible light, Microporous Mesoporous Mater. 134 (2010) 108–114.
[31] A. Nezamzadeh-Ejhieh, M. Karimi-Shamsabadi, Decolorization of a binary azo dyes mixture using CuO incorporated nanozeolite-X as a heterogeneous catalyst and solar irradiation, Chem. Eng. J. 228 (2013) 631–641.
[32] J. Huang, S. Wang, Y. Zhao, X. Wang, S. Wang, S. Wu, S. Zhang, W. Huang, Synthesis and characterization of CuO/TiO_2 catalysts for low-temperature CO oxidation, Catal. Commun. 7 (2006) 1029–1034.
[33] G.D. Moon, J.B. Joo, I. Lee, Y. Yin, Decoration of size-tunable CuO nanodots on TiO_2 nanocrystals for noble metal-free photocatalytic H_2 production, Nanoscale 6 (2014) 12002–12008.
[34] G. Li, N.M. Dimitrijevic, L. Chen, T. Rajh, K.A. Gray, Role of surface/interfacial Cu^{2+} sites in the photocatalytic activity of coupled CuO−TiO_2 nanocomposites, J. Phys. Chem. C 112 (2008) 19040–19044.
[35] E.M. Rodríguez, G. Márquez, E.A. León, P.M. Álvarez, A.M. Amat, F.J. Beltrán, Mechanism considerations for photocatalytic oxidation, ozonation and photocatalytic ozonation of some pharmaceutical compounds in water, J. Environ. Manage. 127 (2013) 114–124.
[36] I. Ibrahim, A. Ismail, R. Mohamed, Degradation of free cyanide by photocatalytic oxidation, Eur. J. Mineral Process. Environ. Protect. 3 (2003) 281–290.
[37] X. Chen, S.S. Mao, Titanium dioxide nanomaterials: Synthesis, properties, modifications, and applications, Chem. Rev. 107 (2007) 2891–2959.
[38] S. Xu, J. Ng, X. Zhang, H. Bai, D.D. Sun, Fabrication and comparison of highly efficient Cu incorporated TiO_2 photocatalyst for hydrogen generation from water, Int. J. Hydrogen Energy 35 (2010) 5254–5261.
[39] X. Zhao, Z. Li, Y. Chen, L. Shi, Y. Zhu, Enhancement of photocatalytic degradation of polyethylene plastic with CuPc modified TiO_2 photocatalyst under solar light irradiation, Appl. Surf. Sci. 254 (2008) 1825–1829.